PERGAMON

Journal of Structural Geology 25 (2003) 1213–1227

JOURNAL OF STRUCTURAL GEOLOGY

www.elsevier.com/locate/jsg

Numerical models for the control of inherited basin geometries on structures and emplacement of the Klippen nappe (Swiss Prealps)

S.B. Wissing*, O.A. Pfiffner

Institute of Geological Sciences, University of Berne, Baltzerstr. 1-3, CH-3012 Berne, Switzerland

Received 19 March 2002; received in revised form 9 September 2002; accepted 27 September 2002

Abstract

Cover nappes commonly deform above a shallow basal detachment surface located above rigid crystalline basement rocks. Inherited basin geometries are presumed to control the kinematic evolution and detachment of cover nappes in an accretionary wedge. We compare results from two-dimensional finite element modelling with the structural style of a natural cover nappe, the Klippen nappe, which was detached from its basement along an evaporitic detachment horizon and thrust over a distance of roughly 100 km. First-order characteristics of the Klippen nappe paleo-basin include a complex distribution of weak detachment rocks and various changes in the sediment composition and layer thicknesses; two types of structural style can be distinguished: an imbricate fan at the rear end of the nappe (Préalpes Médianes Rigides) and a fold-dominated region at the front (Préalpes Médianes Plastiques).

The model results resemble the first-order characteristics of the Klippen nappe. The model experiments suggest that the formation of imbricates and fault-related folds are controlled by the discontinuity of detachment horizons. Discontinuities are locations where thrust ramps are triggered and layer heterogeneities control the locations for the initiation of detachment folds. Basement horsts may lead to the formation of recumbent folds, which develop a mélange zone on the highly sheared inverted limb. The experiments also suggest that the thickness of the basal detachment horizon of the Médianes Plastiques decreases gradually from the foreland to the hinterland.

Keywords: Finite-element models; Inherited basin geometry; Detachment folds; Imbricates; Detachment horizon; Heterogeneities

1. Introduction

Fold-and-thrust belts often exhibit structural styles that reflect the nature of inherited lithic units and lateral heterogeneities caused by, for example, synsedimentary normal faults. The basal thrusts of nappes commonly follow mechanically weak detachment horizons such as evaporite layers or shales. The nappes also undergo nappe-internal deformation.

Folding and thrusting are the main mechanisms by which nappes are internally thickened and shortened. In many cases the basal detachment horizon is located above a rigid crystalline basement near the base of the sedimentary sequences. This style of deformation, in which the basement remains undeformed is referred to as 'thin-skinned tectonics'. The developing nappes are known as 'cover nappes' (Escher et al., 1993; Epard and Escher, 1996).

Changes in structural styles of cover nappes caused by variations in lithologic composition and mechanical stratigraphy are discussed in numerous early and recent studies (Willis, 1893; von der Weid, 1961; Currie et al., 1962; Johnson, 1980; Wiltschko, 1981; Wiltschko and Eastman, 1983, 1988; Schedl and Wiltschko, 1987; Woodward, 1988; Butler, 1989; Woodward and Rutherford, 1989; Fermor and Moffat, 1992; Fischer and Woodward, 1992; Pfiffner, 1993; Sassi et al., 1993). Facies and thickness changes in stratigraphic successions are assumed to influence ramp locations, folding versus thrusting mechanisms and localization of deformation in shear zones and thrust faults.

Cover nappes are typical for the Helvetic and Penninic zones of the Alps. During Mesozoic rifting and subsidence the Alpine sedimentary realm differentiated into basins and topographic highs. Argand (1911) proposed that basement highs and lows inherited from Mesozoic basin development pre-determined the sites of Tertiary compressional deformation, and hence directly influenced the specific pattern of nappes as observed today.

* Corresponding author.
E-mail address: silke.wissing@geo.unibe.ch (S.B. Wissing).

0191-8141/03/$ - see front matter © 2002 Elsevier Science Ltd. All rights reserved.
PII: S0191-8141(02)00159-1

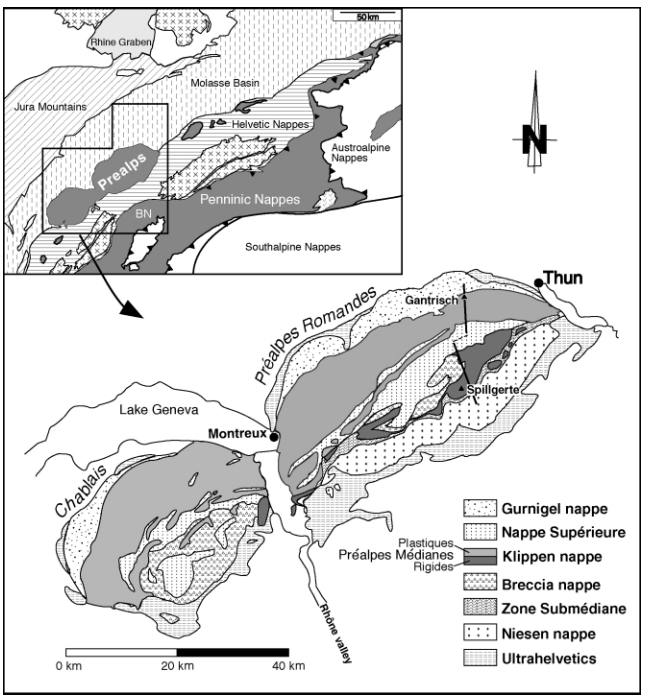

Fig. 1. Tectonic sketch map of the Klippen nappe (Préalpes Romandes and Préalpes du Chablais) and its position within the Alps (inset). BN: Bernhard nappe.

A classic example of this style of inherited basin tectonics is the Klippen nappe, which forms part of the Swiss Prealps (Fig. 1). This nappe roots in the Penninic zone and subsequently travelled far out into the external zone, thereby becoming separated from the internal Alpine basement on which its sediments were originally deposited. In a field study (Wissing and Pfiffner, 2002) we examined the internal deformation of the Klippen nappe. Its Mesozoic carbonate sequence was deposited on the Briançonnais microcontinent and later detached along Late and Middle Triassic evaporites. Some Briançonnais sediments are found in the Bernhard nappe (Siviez-Mischabel and Pontis digitations; Escher, 1988). They remained attached to the basement and underwent Alpine deformation and metamorphism (Sartori, 1987, 1990).

Numerical models of lithospheric deformation can be used to test conceptual ideas about deformation processes. In this paper, we use numerical finite element models to illustrate how factors such as the thickness and continuity of mechanically weak detachment layers, the geometry of carbonate layers, and paleofaults may cause specific styles of deformation in cover nappes. We extend studies from an another work dealing with more generic models of Alpine-type cover nappe deformation (Wissing et al., 2002).

In this study, we consider geometries resembling the Klippen nappe paleobasin, and analyse whether the structural style may have formed as a consequence of geometric properties. The aim is to understand the first-order characteristics of structural styles typical for cover nappes, which evolved from a paleobasin undergoing basal detachment and internal deformation.

2. Natural example in the Western Prealps: the Klippen nappe

The Penninic nappe stack forming the Prealps is located along the northwestern front of the present western Swiss Alps. Two large lobes are formed by the 'Préalpes du Chablais' south of Lake Geneva and the 'Préalpes Romandes' east of Lake Geneva (Fig. 1). Smaller erosional remnants of Penninic nappes are found as 'Klippen' in central and eastern Switzerland (Stanserhorn, Mythen, Grabs) as well as in France (Annes and Sulens) south of Lake Geneva. These Klippen testify that the Klippen nappe was formerly part of an orogenic wedge, which was eroded in the later stage of Alpine orogeny.

In general, the Prealps are subdivided into four units, from top to bottom: (1) Nappe Supérieure, (2) Breccia nappe, (3) Klippen nappe (also known as 'Préalpes Médianes'), and (4) Niesen nappe (Caron, 1972). During Alpine orogeny, this nappe stack detached from its substratum, the distal European continental margin (Niesen nappe), the Briançonnais microcontinent (Klippen and Breccia nappes) and the Piemont ocean (Breccia nappe and Nappe Supérieure) and was incorporated into the accretionary wedge of the closing Piemont ocean (Fig. 2b). The entire nappe stack was then thrust on top of the future Helvetic nappes and even onto the Molasse basin in the north.

The Klippen nappe consists of a Mesozoic carbonate sequence, deposited on the Briançonnais microcontinent. Its low-grade metamorphism resulted from heating due to modest tectonic burial. The burial depth was about 2 km at the northern end and ≤ 10 km at the southern end of the Klippen nappe, according to the studies of Mosar (1988) and Jaboyedoff and Thélin (1996).

Jurassic extensional synsedimentary faults caused an

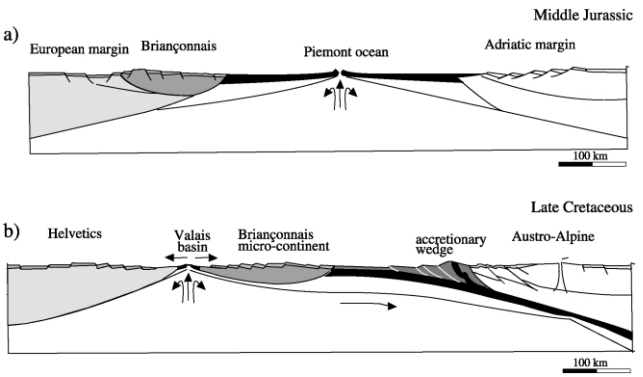

Fig. 2. Schematic cross-sections of the European and Apulian rift margins at (a) Middle Jurassic and (b) Late Cretaceous times. Modified after Marthaler (1998).

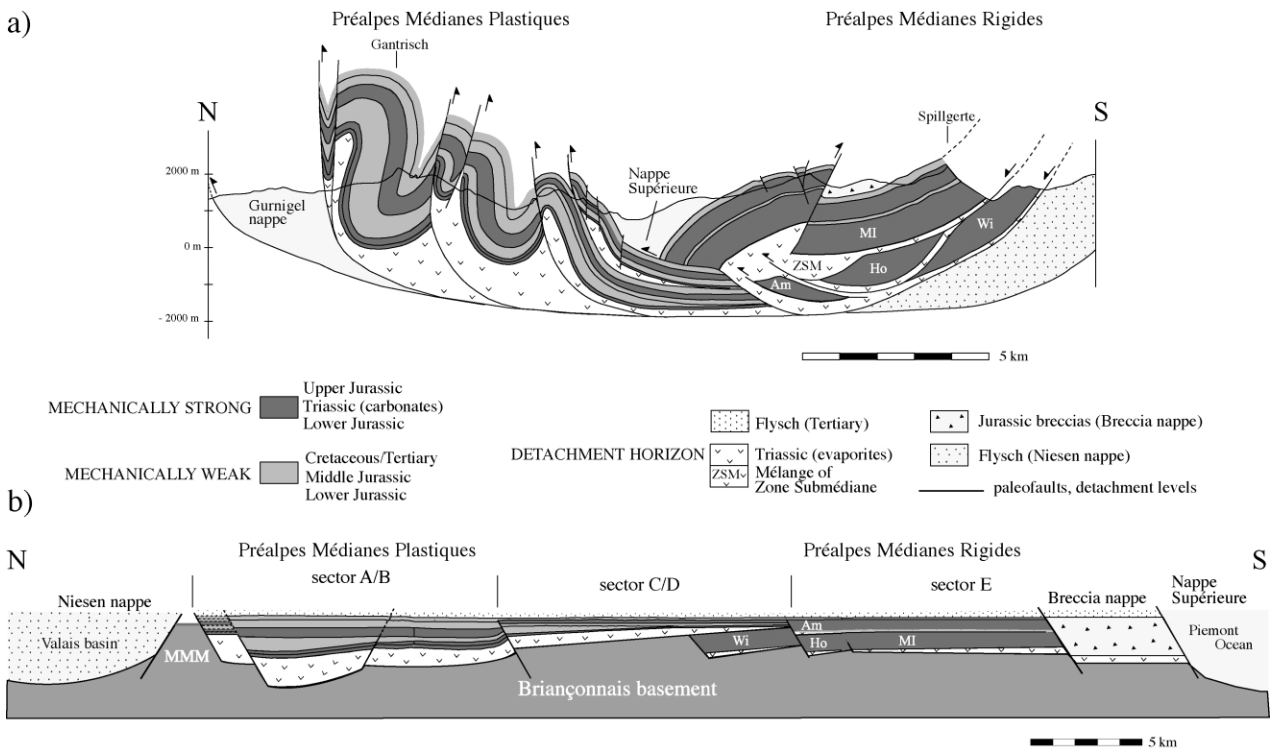

Fig. 3. (a) Synoptic cross-section of the Klippen nappe after Wissing and Pfiffner (2002). For location see Fig. 1. Stratigraphy is simplified by combining competent and incompetent units respectively. (b) Reconstruction of the Klippen nappe paleobasin. Am: Amselgrat/Zünegg imbricate, Ho: Homad imbricate, Wi: Wierihorn imbricate, MI: Main imbricate, MMM: Môle–Moléson–Mythen 'high', ZSM: Zone Submédiane. The width of the MMM-high is not constrained by field data.

irregular distribution of mechanically weak and strong sediments and subsequently influenced the later structure of the nappe during Alpine collision significantly. The main rifting phase, in which the Prealpine basin reached its maximum extension, corresponds to the opening of the Alpine Tethys ocean during Middle Jurassic times (Bill et al., 1997). At that time the Briançonnais microcontinent was located on a rim basin along the northern part of the Alpine Tethys and underwent moderate extension on a rift shoulder (Stampfli, 1993; Stampfli and Marthaler, 1990; Fig. 2a). Related to this rifting event, important synsedimentary faults developed, which divide the Klippen nappe into different facies areas perpendicular to strike. This subdivision of the paleobasin is reflected in the macrotectonic differences noted by Lugeon and Gagnebin (1941), who divided the Klippen nappe into two parts: the 'Préalpes Médianes Rigides' in the south and the 'Préalpes Médianes Plastiques' in the north. This nomenclature paraphrases a change in structural style from a fold-dominated northern part to predominantly large imbricate structures in the southern part of the nappe. It makes an important distinction between two areas with different stratigraphy and structural style (Baud and Septfontaine, 1980).

The detachment horizon of the Prealpine units is composed of an interlayering between dolomite and anhydrite, now transformed to gypsum and rauhwacke. The Klippen nappe has been transported over a distance of more than 100 km (Masson, 1976).

In the following section we give an overview on the most important structural features of the Klippen nappe, which are relevant for a comparison with our model experiments. For a more detailed commentary on the structures and internal deformation of the Klippen nappe the reader is referred to Mosar (1989, 1991, 1997), Mosar and Borel (1992), Plancherel (1979), Wissing and Pfiffner (2002) and references therein.

2.1. The northern part: Préalpes Médianes Plastiques

Carbonate rocks of the Préalpes Médianes Plastiques consist of thick bedded massive carbonates interlayered with marly and shaly units acting as mechanically weaker horizons (Fig. 3). Synsedimentary paleofaults offset the layering and are responsible for thickness and facies changes. The style of deformation related to this multilayered sequence is characterized by large scale, en échelon fold structures. Folds are detachment folds (in the sense of Jamison (1987)), and the fore-limbs are often cut by thrust faults. The simplified retrodeformed basin geometry of the Klippen nappe (Fig. 3b) shows that the positions of these thrust faults in many cases coincide with irregularities

(offsets and/or facies changes) along synsedimentary paleofaults.

The reduced thicknesses of the carbonates in the external part of the basin are interpreted to be related to a topographic basement high (the Môle–Moléson–Mythen, or MMM-high; Boller, 1963) at the northern end of the Médianes Plastiques paleobasin, which separates the Briançonnais realm from the Valais trough (Niesen nappe; Fig. 3b).

The basal thrust of the Préalpes Médianes Plastiques steepens to a vertical orientation at the contact to the Gurnigel nappe. The Gurnigel nappe is regarded as a digitation of the overlying Nappe Supérieure (Caron et al., 1980), which had been cut off and overthrust by the Préalpes Médianes in a later stage of deformation (out-of-sequence thrusting; Wissing and Pfiffner, 2002).

In a general way, the structural style of the Médianes Plastiques is in good agreement with the observations of Willis (1893) in the Appalachians and the model results of Currie et al. (1962), Chester et al. (1991), Fermor and Moffat (1992) and Wissing et al. (2002), all of whom emphasized the importance of multilayered sequences on the evolution of fold structures.

In the following we discuss a series of model experiments designed to investigate fold evolution in the Préalpes Médianes Plastiques during compression and transport across a topographic basement high (MMM) at their northern boundary. The experiments provide insight into the influence of offsets in both sediment layering and the basement below on the formation of folds and related thrusts.

2.2. The southern part: Préalpes Medianes Rigides

In comparison with the northern part of the nappe, the Préalpes Médianes Rigides contain much more thick and massive carbonates. The thick middle Jurassic units and the lower Cretaceous rocks are missing. Massive late Jurassic platform carbonates are underlain by thick bedded Triassic carbonates and limestones. Only a thin middle Jurassic member separates these competent units. The thickness of the evaporite detachment layer is thinner as compared with the northern part. According to the studies of Johnson (1980), Wissing et al. (2002) and Woodward (1988), such mechanically strong and thick layers tend to form imbricates rather than folds. This phenomenon is clearly expressed in the structural style of the Médianes Rigides, which is characterized by large rigid imbricates (Fig. 3a).

One large thrust sheet with a complete sequence from middle Triassic to upper Cretaceous rocks dominates the style. We refer to this imbricate with its complete Mesozoic sequence as the 'Main imbricate' (MI). It is underlain by one or more smaller scaled imbricates, which are separated from the overlying Main imbricate by evaporites and mélange material of the Zone Submédiane (ZSM). The 'Wierihorn' (Wi) and Homad (Ho) imbricates consist of middle and upper Triassic carbonates only. The Amselgrat/Zünegg lens (Am) contains mainly upper Jurassic rocks. Both the Homad and the Amselgrat imbricates pinch out quickly to the northeast and southwest and are interpreted as large boudin-like, lens-shaped components of the Zone Submédiane (Wissing and Pfiffner, 2002).

Thrust faults in the Préalpes Médianes Rigides are now dipping to the NW owing to rotation in the course of later compressional events in the underlying Helvetic zone.

2.3. The detachment layers

The base of the Klippen nappe consists of a sequence of initially interlayered anhydrite–dolomite deposits. Due to the very low shear resistance of anhydrite, this layer acted as a detachment horizon for the overlying sediments. Today these evaporitic rocks outcrop along tear and thrust faults and within the mélange zones (e.g. Zone Submédiane), often extensively altered to rauhwacke.

The basal detachment of the Klippen nappe is located at two different stratigraphic levels. In the Médianes Plastiques, the evaporites are of late Triassic (Carnian) age. In contrast, the carbonates of the Médianes Rigides were decoupled from the basement at a deeper level, along middle Triassic evaporites (Fig. 3b). The Préalpes Médianes Rigides therefore include thick bedded middle Triassic carbonates, which are absent in the Préalpes Médianes Plastiques.

The existence and continuity of a weak detachment horizon is regarded to be one of the important controlling features on the structural style and transport width of cover nappes. Large displacements and folding within a nappe is only possible if the internal deformation and decoupling of the nappe is accomodated by a sufficient thickness of weak layers (Pfiffner, 1993). In addition, the generic models of Wissing et al. (2002) and the work of Willis (1893) and Rodgers (1950) suggest that a thick detachment horizon (relative to nappe sediment thickness) favours a fold-style of deformation, while a thin detachment horizon leads to the formation of imbricates.

The thickness of the evaporites beneath the Prealps is not well constrained, but varies across the nappe. In the north, the Médianes Plastiques, it is possibly in excess of 1000 m according to seismic data (Wissing and Pfiffner, 2002). In the southeast, the Médianes Rigides, it is less than 500 m. The detachment horizon is disrupted by Jurassic paleofaults. The associated lateral heterogeneity will be discussed in detail in the context of the experiments. The absence of mechanically weak rocks in some parts of the basin may have resulted in the coupling of sediments to their Briançonnais basement, whereas other parts were detached and transported to the NNW (Baud and Septfontaine, 1980; Sartori, 1990).

3. Model study

We use two-dimensional finite element models to investigate deformation at the scale of a cover nappe in response to boundary conditions representing a simplified accretionary wedge. Before we present results of model experiments, we discuss the justification for the geometry and material properties used in the models, and modelling limitations.

3.1. Model boundary conditions and limitations

We use the two-dimensional finite element code MICROFEM (developed by Philippe Fullsack from the Dalhousie Geodynamics Group in Halifax, Canada), which solves for force equilibrium and includes brittle plastic (Coulomb) as well as viscous rheology, to examine the behaviour of our cover nappe material under compression. The code uses two grids with quadrilateral elements. To prevent problems with highly sheared elements and to allow large deformation to occur, calculations are performed on an Eulerian grid, in which the grid elements only stretch vertically. Tracking of interfaces and material properties is carried out using a Lagrangian grid. For further details of the arbitrary Lagrangian–Eulerian technique and the numerical method, the reader is referred to Fullsack (1995).

In order to investigate the dynamics that led to the formation of the Klippen nappe, we have simplified the geometry of the orogenic wedge (Fig. 4a), which evolved from accretion and nappe transport as follows: in Eocene times, the Nappe Supérieure, which contains flysch-type sediments, was emplaced onto the Klippen nappe. Next, the Klippen nappe was incorporated into the upper plate orogenic wedge, which contained oceanic siliciclastic sediments of the closing Piemont ocean. For a detailed discussion of the evolution of the Penninic nappe stack, the reader is referred to Trümpy (1960), Lemoine et al. (1986), Stampfli and Marthaler (1990), Mosar (1991), Mosar et al. (1996), Pfiffner et al. (1997) and references therein.

The model setup we chose to reflect a simplified initial model basin geometry is given in Fig. 4b–d for individual experiments presented here. The general geometry of the simple model accretionary wedge is a tapered block of Coulomb-frictional wedge material with an upper unit of model flysch nappes overlying a model nappe made up of sediments and an evaporite detachment layer (area of interest).

We assign a linear viscous rheology with a coefficient of viscosity of $\eta = 10^{20}$ Pa s to the detachment layer and a brittle-plastic rheology to both wedge sediments and competent carbonate layers. The competent carbonates of the Klippen nappe are set to an angle of internal friction of 15°, the incompetent interlayers within the Klippen nappe, the overlying nappes and the upper plate orogenic wedge have a less competent brittle-plastic rheology with an angle of internal friction of $\phi = 12°$. These values for internal friction are set deliberately lower than values measured in laboratory experiments (Byerlee's law) and than estimates from critical taper studies, to implicitly include effects of ambient fluid pressure (Beaumont et al., 1996). The existence of a pore fluid is demonstrated by the presence of numerous calcite filled veins within folds and in the vicinity of thrust faults within the Klippen nappe. The effect of varying friction angles is discussed in more detail in Wissing et al. (2002).

Cohesion is set to the relatively low value of 10 MPa in all frictional layers, density is 2800 kg m^{-3}. Test runs with lower density values of 2200 kg m^{-3} for the linear viscous layer, as well as test runs with higher cohesion values for the brittle-plastic layers show similar results.

To simulate convergence, material is brought in from the right hand side of the model at a rate of 1 cm a^{-1}. The base of the model moves with a constant velocity up to a detachment point (black dot). From this point to the left the base of the model is held fixed. The abrupt change in basal velocity at this position is a convenient and simplified representation of the inferred detachment of the Klippen nappe at a 'zone of minimum channel capacity' (terminology of Shreve and Cloos, 1986). The area of interest is assumed to have detached at or prior to crossing this point.

The left hand model boundary is held fixed with only vertical movements of nodes allowed. This does not correctly simulate the effect of a semi-infinite sheet and therefore the models are constructed to keep the main portion of deformation away from this boundary. Behaviour of the crust in deeper levels below the detachment horizon is represented by a zero-velocity boundary condition at the base of the model domain, where neither horizontal nor vertical movement of nodes is permitted. This simulates a high strength contact between the stratigraphic pile and a rigid basement.

We focus on upper crustal scale deformation of sedimentary rocks in shallow depths. Only the top 6.5 km of the crust is modelled. Processes in the lower crust, mantle and the subduction zone itself are not taken into account. The geometry and taper angle of the wedge is chosen to be close to critical in order to minimize the development of strain on the wedge side of the model and optimize the amount of deformation in the area of interest (Wissing et al., 2002).

The nodes at the hinterland boundary may move vertically while the boundary is displaced to the right as a vertical plane. The top boundary (representing the Earth's free surface) is free to move in any direction within the model plane.

The total thickness at the left boundary is 2.5 km, the maximum initial wedge thickness at the right hand boundary is 6.5 km. This wedge geometry accounts for the higher burial depths observed in the Préalpes Médianes Rigides compared with the Préalpes Médianes Plastiques. The overall width of the model domain is 120 or 100 km, but the significant part of deformation occurs in a smaller model

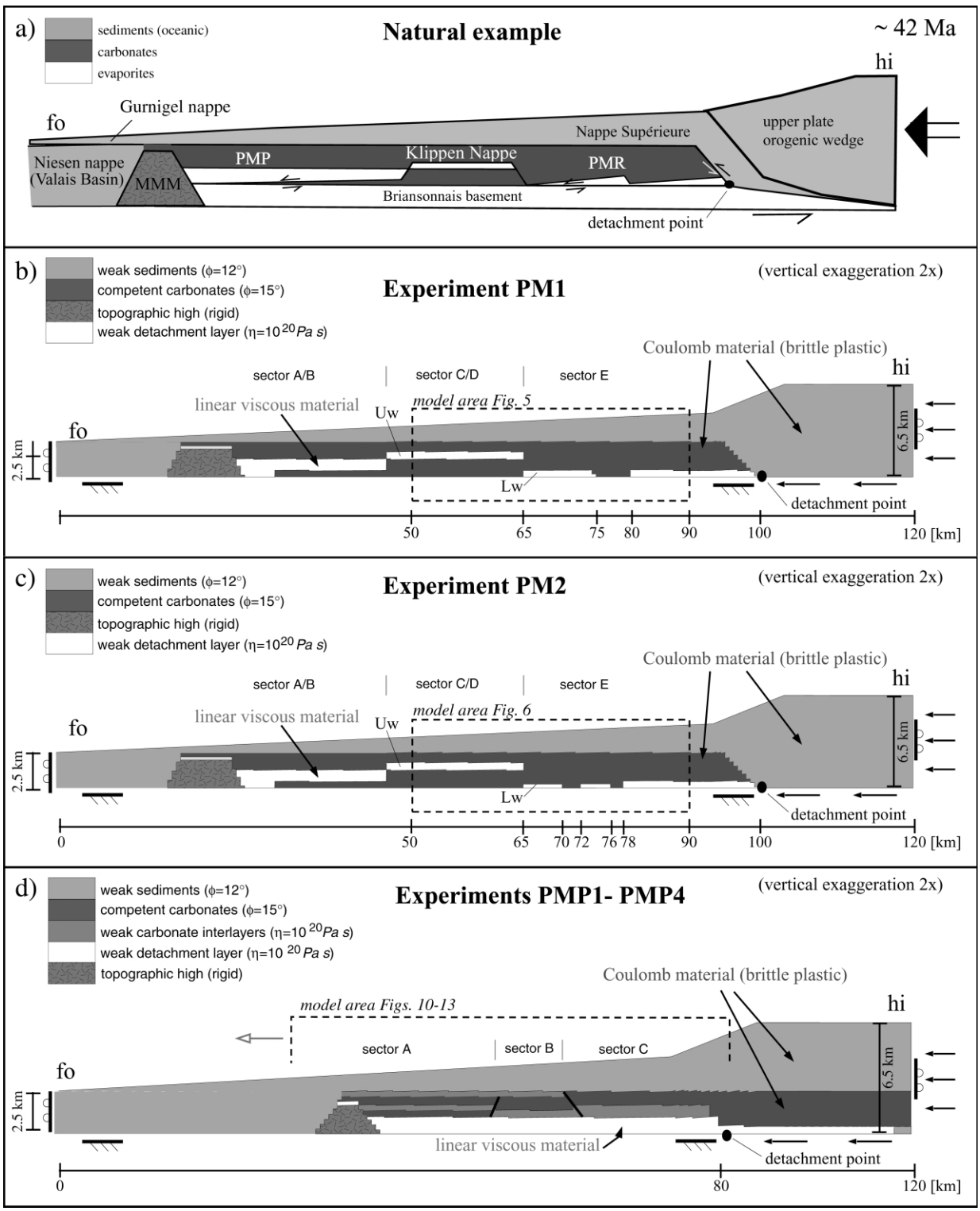

Fig. 4. (a) Schematic setup of Klippen nappe deformation. The black dot stands for the detachment point, the position where overlying units presumably detached from their basement (see text). fo, hi: foreland and hinterland sides of the orogenic wedge. MMM: Môle–Moléson–Mythen 'high'. PMP: Préalpes Médianes Plastiques, PMR: Préalpes Médianes Rigides. Material properties, no tracking grid. (b) Model setup of experiments PM1 (Fig. 6). (c) Model setup of experiments PM2 (Fig. 7) Lw: 'Lower weak layer', Uw: 'Upper weak layer' (see text). (d) Model setup of experiment PMP1. Experiments PMP2–PMP4 generally use the same setup with specific differences outlined in the text and the figure captions of Figs. 10–12. Note that model areas displayed in Figs. 9–12 move forward with convergence (arrow).

portion, to prevent influences of the model boundaries. Deformation taking place at the right-hand boundary (within the wedge sediments) is neglected.

The models are designed to show the important controlling factors in a basin environment under compression. Due to limited displacement and resolution of models, they are not meant to record or reproduce small scale structures and emplacement in detail. Small scale heterogeneities and processes are poorly resolved in these models and it is important to keep the geometry of the models as simple as possible and consider large scale processes only. For the models shown in this paper, resolution is 201 node points horizontally by 61 nodes vertically. Tests with the same geometry but doubled grid resolution (401 by 121 node points) do not change the overall results, but need much more computation time.

Sedimentary rocks deformed at shallow conditions are a brittle, frictional material. Failure in such a material in many cases occurs as shear on discrete planes. This material can be described approximately with a plastic rheology following a Coulomb–Mohr failure criterion (Handin, 1969). A more correct rheological description of the rock model material would have to include elasticity as well as time-dependent failure and strain-dependent (strain hardening/softening) behaviour.

All models are strictly two-dimensional, variations parallel to strike are not considered. Experiments do not investigate the effects of erosion and sedimentation during deformation.

The accreted material maintains the same frictional and viscous strength parameters throughout each model run, although the strength of frictional materials increases with pressure and therefore depth of burial. Changes in rheological mechanisms are not accounted for in the models. The sensitivity of model results due to physical properties are discussed in Wissing et al. (2002) and are interpreted to be uncritical for investigations presented in this paper.

The code is not able to produce discrete zones of failure. On the other hand, the code allows us to obtain a highly strained Lagrangian grid thanks to the arbitrary Lagrangian–Eulerian technique (Fullsack, 1995) mentioned above. Generally there is no standardized criterion to define a thrust fault, but localized zones of highly sheared Lagrangian grid elements are interpreted as shear or fault zones.

The total convergence in the natural analogue is much larger than in our numerical models. Transport width of the Klippen nappe is assumed to be about 100 km, but structures developing during nappe transport over more than 60 km are not investigated in the models presented here.

In this study we intend to show the main features that develop in models with a specific initial geometry, rather than to make quantitative statements about transport width and intensity of deformation in distinct parts of the modelled nappe.

3.2. Experiments

Initial geometries of individual model experiments are described in Fig. 4b–d.Experiments PM1 and PM2 shown in Fig. 4b and c consider the effect of discontinuous detachment layers. Experiments PMP1–PMP4 include multilayers above a continuous detachment horizon, which are disrupted by ‘paleo-faults’ and butt against a rigid ‘basement high’ (Fig. 4d). All model results are illustrated using the material properties and the Lagrangian tracking grid, which gives a description of the finite deformation. Not all node points are displayed; only every third line is plotted. Models are presented in terms of absolute convergence (Δx).

3.2.1. Generic experiments

Wissing et al. (2002) demonstrated that a thick bedded carbonate overlying a thin detachment horizon tends to produce imbricate structures, whereas a carbonate sequence overlying a thick detachment horizon results in detachment folds (their figs. 10 and 11). Detachment folding corresponds to the situation in the Préalpes Médianes Plastiques, imbricate thrusting to the Préalpes Médianes Rigides. Additional factors that influence the formation of imbricates, folds and fault-related folds are investigated in the following sections. We consider models referring to structures in the northern part of the Klippen nappe separately from those relating to deformation in the southern part. The intention is to maintain a maximum balance between complexity and limited resolution of models and to keep model displacement at an appropriate level. We first compare models regarding the formation and stacking of imbricates above thin mechanically weak detachment layers to the conditions we observe in the Préalpes Médianes Rigides (models PM1 and PM2). The second part deals with the formation of folds and thrusts in interlayered carbonates separated by lateral heterogeneities below and within the model layers (models PMP1–PMP4). We then compare these model results with the detachment fold structures observed in the Préalpes Médianes Plastiques.

3.2.2. Experiments PM1, PM2: stacking of imbricates above discontinuous weak layers

Thrusts and ramps appear to seek locations and orientations that provide even a modest reduction in resistance to slip (Davis and Engelder, 1985). It is thus logical to expect that the geometry and distribution (continuity) of weak layers in a basin have a major effect upon the deformation in a cover nappe. The model setup of experiment PM1 accounts for the following conditions of the Médianes Rigides: the evaporites are thin and located in a stratigraphic level below thick competent (middle Triassic) carbonates (Fig. 3b). The detachment horizon at this level is discontinuous owing to Jurassic normal faulting.

We investigate the influence of this thin discontinuous detachment horizon on the development of imbricates in our

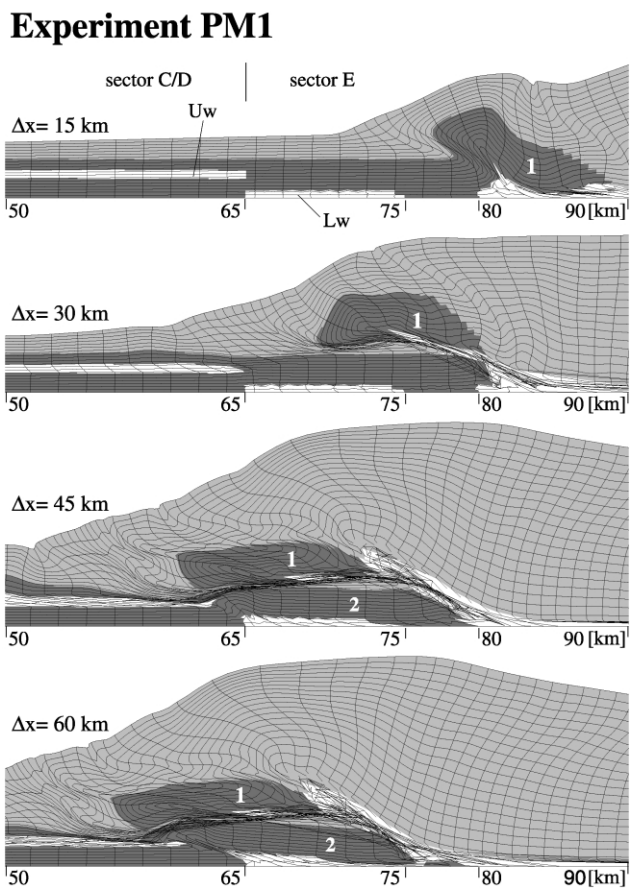

Fig. 5. Model sections of experiment PM1 between 50 and 90 km after different stages of convergence (Δx). Sectors correspond to the sectors indicated in Fig. 3. Lw: 'Lower weak layers', Uw: 'Upper weak layers'.

models. The complete initial setup area of experiment PM1 (Fig. 5) is shown in Fig. 4b. We refer to the different stratigraphic levels of weak detachment material as 'Upper weak' (Uw) and 'Lower weak' (Lw) layers.

The model area shown in Fig. 5 lies between 50 and 90 km, in the trailing part of the model. A relatively thin 'Lower weak layer' (500 m) starts at 100 km and extends up to 80 km. Between 80 and 75 km no mechanically weak material exists, competent brittle model carbonates lie directly on top of the fixed model bottom. Between 75 and 65 km, a second 'Lower weak layer' of the same thickness follows in the direction of the foreland. The evolution in time of experiment PM1 shows how the discontinuity of the mechanically weak material influences the formation of imbricates. Model sections are shown after 15, 30, 52.5 and 60 km of convergence.

At the termination of the first (rear) 'Lower weak layer', an imbricate (**1**) is decoupling from its footwall and is thrust to the foreland under formation of a ramp anticline (15 km convergence). The ramp is located where the weak material terminates and where competent carbonates are coupled to their base. After 30 km of displacement, imbricate **1** is transported on top of the sediments in front. Deformation propagates further to reach the 'Upper weak horizon' in front and through the second 'Lower weak layer'. As deformation reaches the end of the 'Lower weak layer' (52.5 km of convergence), a second imbricate (**2**) starts to decouple at this position. At the same time, the relatively thin competent layer above the 'Upper weak layer' is sheared off from the carbonates in the hinterland and is transported towards the foreland. Imbricate **2** is further removed from its footwall and thrust towards the foreland, carrying the overlying model sediments piggy-back. The carbonates from the position between 75 and 80 km (60 km convergence) are dragging behind. A small piece of cover sediments remains fixed on top of its footwall, where detachment material is absent (between 75 and 80 km). The carbonate layers that exist from 65 to 50 km remain attached to their base.

The reconstruction of the Médianes Rigides paleobasin (Fig. 3b) suggests specific locations for the decoupling of imbricates from their footwall. It postulates two superimposed weak layers below sector C/D. Experiment PM2 (Fig. 6) accounts for these conditions prescribed by our natural analogue, the model deatchment layers are arranged in a similar way as described in the reconstruction of the Médianes Rigides paleo-basin (see Fig. 3). It has the same

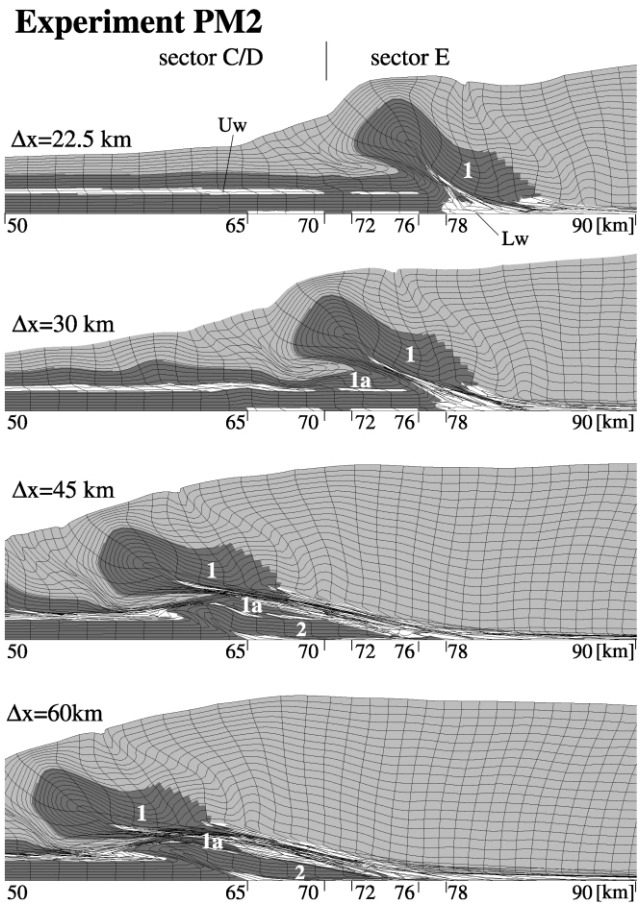

Fig. 6. Model sections of experiment PM2 between 50 and 90 km after different stages of convergence (Δx). Sectors correspond to the sectors indicated in Fig. 3. Lw: 'Lower weak layers', Uw: 'Upper weak layers'.

properties, geometry and boundary conditions as PM1, except that the weak detachment layers are arranged differently and are thinner. This decrease in the thickness of the weak layers is a consequence of the increased complexity of the model domain and the resulting space problems. It does not change their general influence. The trailing part of experiment PM2 shows two superimposed weak layers in the rear part of sector C/D, two additional superimposed thin detachment layers in sector E, and a single 'Lower weak layer' at the hinterland end of sector E.

Experiment PM2 illustrates the following structural evolution in the model domain (50–90 km): imbricate **1** develops as a ramp anticline thrust over the competent rocks in front, in a manner similar to that in experiment PM1 (22.5 km of convergence). After 30 km of convergence, the rear end of sector C/D is sheared and decoupled along the 'Upper weak layer' by the forward motion of material from behind. At the base of imbricate **1**, the small lens **1a** decouples from its footwall (45 km of convergence). At the base shearing reaches the front of the 'Lower weak layer' and the decoupling of imbricate **2** is initiated. After 60 km of convergence, imbricate **2** is thrust over the competent model rocks in front and, together with overlying units, is transported towards the foreland.

These results demonstrate similar conditions to those suggested in a sketch of the evolution of the Médianes Rigides deformation presented in Wissing and Pfiffner (2002). As shown in Fig. 7, the Main imbricate (MI) is thrust over its footwall and forms a ramp anticline along thrust **1** (equivalent to model imbricate **1**; Fig. 6). Continued shortening activated the detachment levels **1a** and decoupled the small Amselgrat lens (Am) from its footwall (equivalent to model imbricate **1a**; Fig. 6). With deformation proceeding, the thin carbonate sequences of sector C/D are transported to the foreland along an upper weak evaporitic horizon. (**2a** and **2b** in Fig. 7). At the same time, decoupling of the Wierihorn imbricate (Wi) is initiated along a lower weak evaporite horizon beneath sector C/D (**2c**, equivalent to model imbricate **2**; Fig. 6). We suggest that the footwall block of the Wierihorn imbricate remained attached to the Briançonnais basement and is preserved in the Pontis digitation of the Penninic Bernhard nappe (BN in Fig. 7). This digitation contains a sequence of gypsum, marbles and dolomites, which can be regarded as the metamorphosed equivalents of the middle to upper Triassic carbonates of the Wierihorn imbricate. We interpret the footwall blocks below imbricate **2** in experiments PM1 and PM2 as equivalents to these remnants of Briançonnais cover sediments that remained attached to the basement. Between 30 and 60 km of convergence in experiments PM1 and PM2, weak sediments from the top of the model carbonates, are overthrust and brought into a position below imbricate **1**, which is regarded to be equivalent to the position of the Zone Submédiane in our natural analogue. This observation is consistent with the study of Dall'Agnolo (1997), who recognized components of the Nappe Supérieure within the Zone Submédiane mélange.

The entire Klippen nappe was detached from its substratum and transported northward along detachment layers, which were located at two different stratigraphic levels. Fig. 8 shows an overview of the complete deformed model domain of experiment PM1 after 60 km convergence and gives an insight into the possible course of nappe decoupling and its transport towards the Alpine foreland. From a topographic high (MMM) in the foreland up to the hinterland end of sector C/D, a detachment horizon thinning towards the hinterland is inferred. It is disrupted by faults extending into the competent material below (see also Fig. 4b). In sector E, decoupling of imbricates occurs along the 'Lower weak layers'. The 'Upper weak layer' is missing in this part of the basin or negligibly thin. As deformation reaches the weak layer in sector C/D, the model carbonates of this sector become cut off from the hinterland. Decoupling along the weak layer leads to internal deformation and transport of the model carbonates towards the foreland. The relatively thick detachment horizon allows the development of detachment folds in this part of the nappe. Deformation runs against a rigid backstop (MMM), which initiates an anticline directly at the 'basement high' and causes the basal thrust to rise and overstep the high. Thrusting of the entire model nappe across the MMM backstop and on top of the sediments of the neighbouring Valais trough (Niesen nappe) is initiated. Carbonates below the upper detachment horizon, in sector C/D, remained attached to their substratum (BN in Fig. 8).

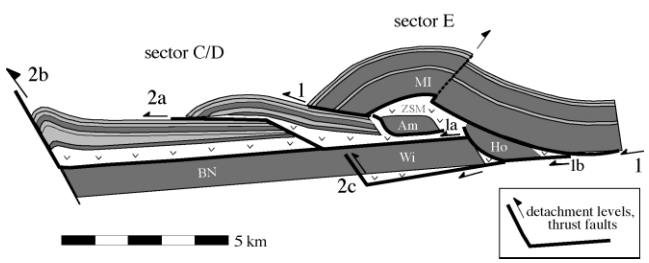

Fig. 7. Scheme of nappe internal deformation of the Préalpes Médianes Rigides. Am: Amselgrat/Zünegg lens, Ho: Homad imbricate, Wi: Wierihorn imbricate, MI: Main imbricate, BN: Mesozoic carbonates which are interpreted to be incorporated into the Penninic Bernhard nappe. Shading and patterns as in Fig. 3.

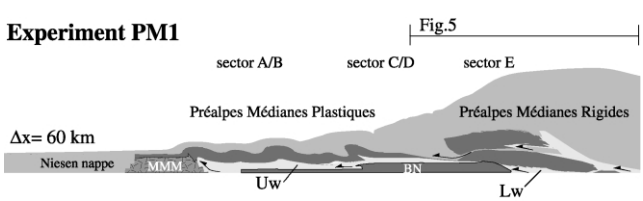

Fig. 8. Interpreted section of experiment PM1 with respect to Klippen nappe detachment. Material properties, no tracking grid. Arrows indicate direction of detachment and thrusting. Model area shown: 0–63 km. Sectors correspond to the sectors indicated in Fig. 3. Lw: 'Lower weak layers', Uw: 'Upper weak layers'.

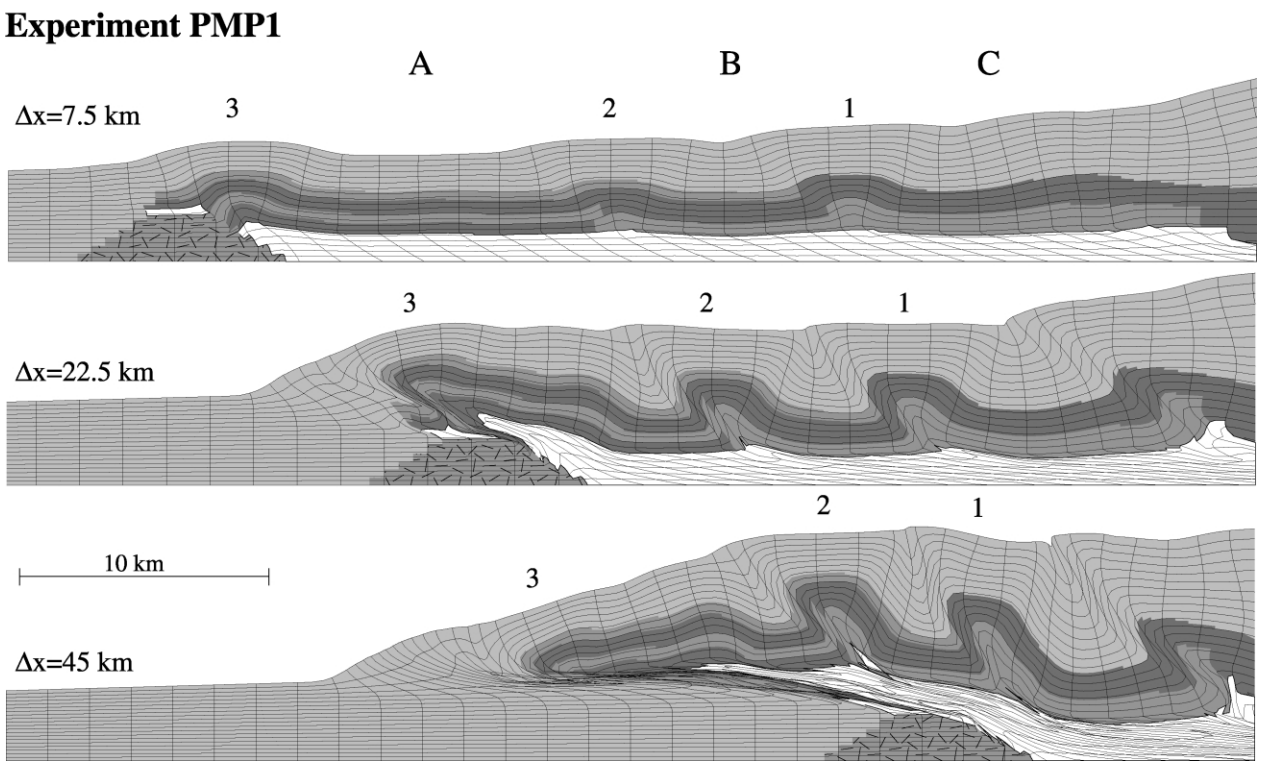

Fig. 9. Sections of experiment PMP1 at different stages of convergence. Area shown extends from: 28–73 km (7.5 km of convergence), to 18–61 km (22.5 km of convergence), to 1–46 km (45 km of convergence). 1, 2, 3: numbers of folds initiated from hinterland to the foreland.

We suggest the results of experiment PM1 to show many of the first order characteristics of the structural style and evolution of the Klippen nappe. In the next following section we will pick up the discussion about deformation of the multilayered sediments of sectors A/B of the Préalpes Médianes Plastiques, its fault-related fold structures and its transport across a rigid 'basement' high.

3.2.3. Experiments PMP1–PMP4: folds and related thrust faults in heterogeneous multilayered material

In the Préalpes Médianes Plastiques, the thickness of the basal detachment layer of the Klippen nappe sediments likely is relatively large (Fig. 3). The carbonate units consist of competent limestones interlayered with mechanically weaker, more marly sequences. Jurassic synsedimentary normal faults separate sectors of carbonate sequences of different composition and thickness. The boundaries between these sectors therefore form important heterogeneities and discontinuities.

We set up a model geometry that includes both interlayered model rocks and irregularities (offsets) within the sequences to investigate the influence that such irregularities may have on fold formation and the evolving fold train pattern in carbonate multilayers. The initial model geometry is illustrated in Fig. 4d for experiment PMP1. Specific changes implemented for the additional experiments PMP2–PMP4 are explained in the text and the figure captions of Figs. 11 and 12.

Three individual sectors with different numbers and thicknesses of interlayered mechanically strong and weak brittle-plastic units are included for each model. The angle of internal friction of the weak interlayers is (for simplicity) the same as for the wedge material ($\phi = 12°$). The complexity of multilayer geometry is limited by model resolution and represents an oversimplification of conditions of naturally multilayered rocks, which normally consists of a larger number of individual layers. The model geometry of layers and related paleofaults is a compromise between real conditions and the attempt to provide numerically significant heterogeneities in the model.

Sector A (see Fig. 4d) consists of an interlayering between two weak and two competent units. Sector B contains two weak layers, one at the top and one at the bottom of a single competent unit. Sector C incorporates only two layers, a competent and a mechanically weaker brittle-plastic unit. The paleofault between sector A and B is inferred to be foreland dipping, whereas the paleofault between sector B and C dips in the direction of the hinterland. The 'basement' high MMM is inserted into the model geometry as a rigid horst. The area to the left of the horst consists of weak brittle-plastic sediments. The wedge side of the experiment has a competent plastic layer moving in from the right-hand side, simulating a rigid sediment body (Médianes Rigides) pushing from behind. We inserted a weak linear viscous layer at the base of the wedge, to lower the basal friction of the wedge and to account for mechanically weak material available at the base of the rocks in the hinterland. High strength contrasts

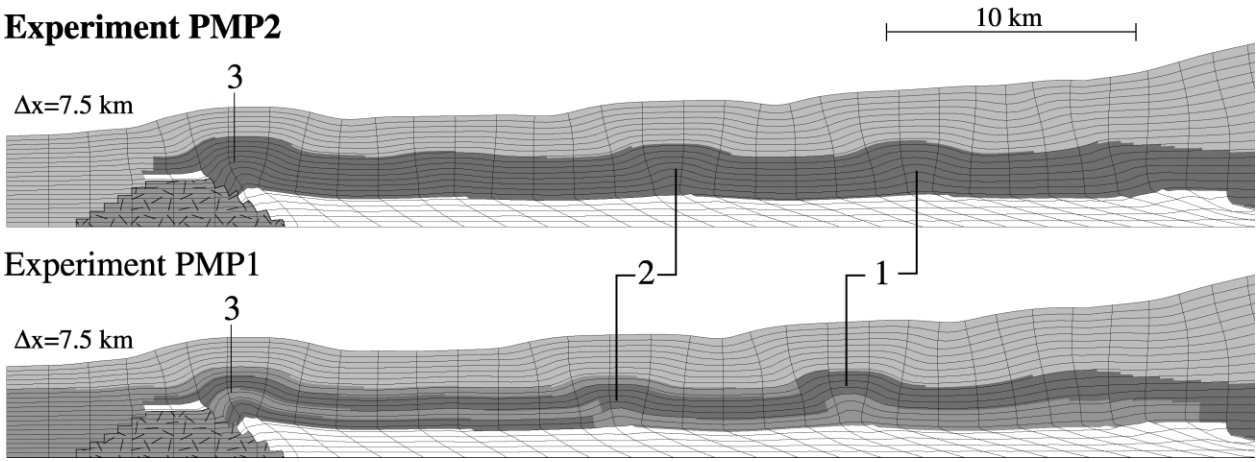

Fig. 10. Sections of experiment PMP2 and PMP1 after 7.5 km of convergence. Area shown extends from: 28–73 km. 1, 2, 3: numbers of folds initiated from hinterland to the foreland.

lead to numerical instabilities at the right hand boundary of models and therefore the linear viscous layer is replaced by a somewhat stronger weak brittle-plastic layer ($\phi = 12°$) close to the boundary (see Fig. 4d).

After compression of this model geometry (experiment PMP1), the following observations can be made (Fig. 9): after 7.5 km of convergence, detachment folds are initiated above the relatively thick weak linear viscous layer. Anticlines are located directly at (or behind) the discontinuities between units (**1**, **2**) or behind the rigid horst (**3**).

As deformation continues, the model paleofaults **1** and **2** are preferred positions for the localization of deformation in the forelimb of detachment folds. Juxtaposed weak horizons are used as favoured slip planes (see fold **2**, after 22.5 km of convergence).

A strongly inclined frontal fold (3) forms above the rigid horst. It pushes the weak layers on top of the horst towards the left, and drags them towards the foreland. The overturned limb of this frontal fold is intensely sheared. The amount of strain localization in the forelimbs of all three folds increases with increasing displacement. After 45 km of convergence, the frontal fold becomes recumbent with only the backlimb preserved. The small remnants of the forelimb and the thin carbonate sequence from the top of the horst are preserved below the base thrust of fold **3**, but are invisible in Fig. 9 due to the intensely sheared grid elements.

Experiment PMP2 has the same geometry as PMP1, but the entire multilayered sequence is replaced by one single strong layer in order to investigate the differences in early stage of fold initiation (Fig. 10). As would be expected, multilayered experiment PMP1 shows a higher fold amplitude after 7.5 km of convergence (compare folds **1** and **3** in both experiments). The positions of initial folds in experiments PMP1 and PMP2, however, is not the same: folds **1** and **2** in PMP2 are generated closer to the hinterland compared with folds **1** and **2** in PMP1. Positions of initial folds are generally controlled by strength and thickness contrasts between the plastic layers and the linear viscous layer (Wissing et al., 2002), and should therefore not be much different in both experiments. We interpret that in the case of PMP1, the paleofaults give rise to perturbations and thus influence the wavelength pattern of folded layers.

Experiment PMP3 considers a decrease in the thickness of the weak detachment horizon towards the hinterland, accompanied by offsets in the underlying rigid substratum (Fig. 11). Strong layers with a model carbonate rheology (brittle-plastic, $\phi = 15°$) are inserted below the weak linear viscous layer, which produces offsets in the weak layer directly at the downward projected continuation of paleofaults. This simulates a continuation of these faults into the competent layers below (middle Triassic carbonates in the case of the Klippen nappe). All other conditions are equal to experiment PMP1, which is displayed along with PMP3 for comparison. Both experiments show initiation of folds at layer heterogeneities. After 7.5 km of convergence, experiment PMP3 developed fold **1**, while experiment PMP1 (with a thicker detachmnet layer) developed folds **1** and **2**. After 22.5 km of convergence, folds **1** (of PMP1 and PMP3) have attained different geometries. In PMP3, the perturbations related to the basement step (visible as inhomogeneously distorted grid elements just to the right of the basement step) have created a new fold to the left of the model paleofault. After 45 km of convergence, the paleofault is located on the backlimb of fold **1** in the case of PMP3, while it is on the forelimb for PMP1.

Such perturbations in the weak detachment layer have been reported from model studies of Schedl and Wiltschko (1987), Wiltschko and Eastman (1983, 1988) and Wissing et al. (2002), who related them to perturbations in the stress field. It seems that stress perturbations at basement steps have a major impact on strain localization. They control the evolution of individual strain patterns within a fold train and are able to suppress potential folds at lateral layer heterogeneities.

In experiment PMP4, the abrupt basement steps beneath the weak detachment layer are replaced by a shallow dipping ramp

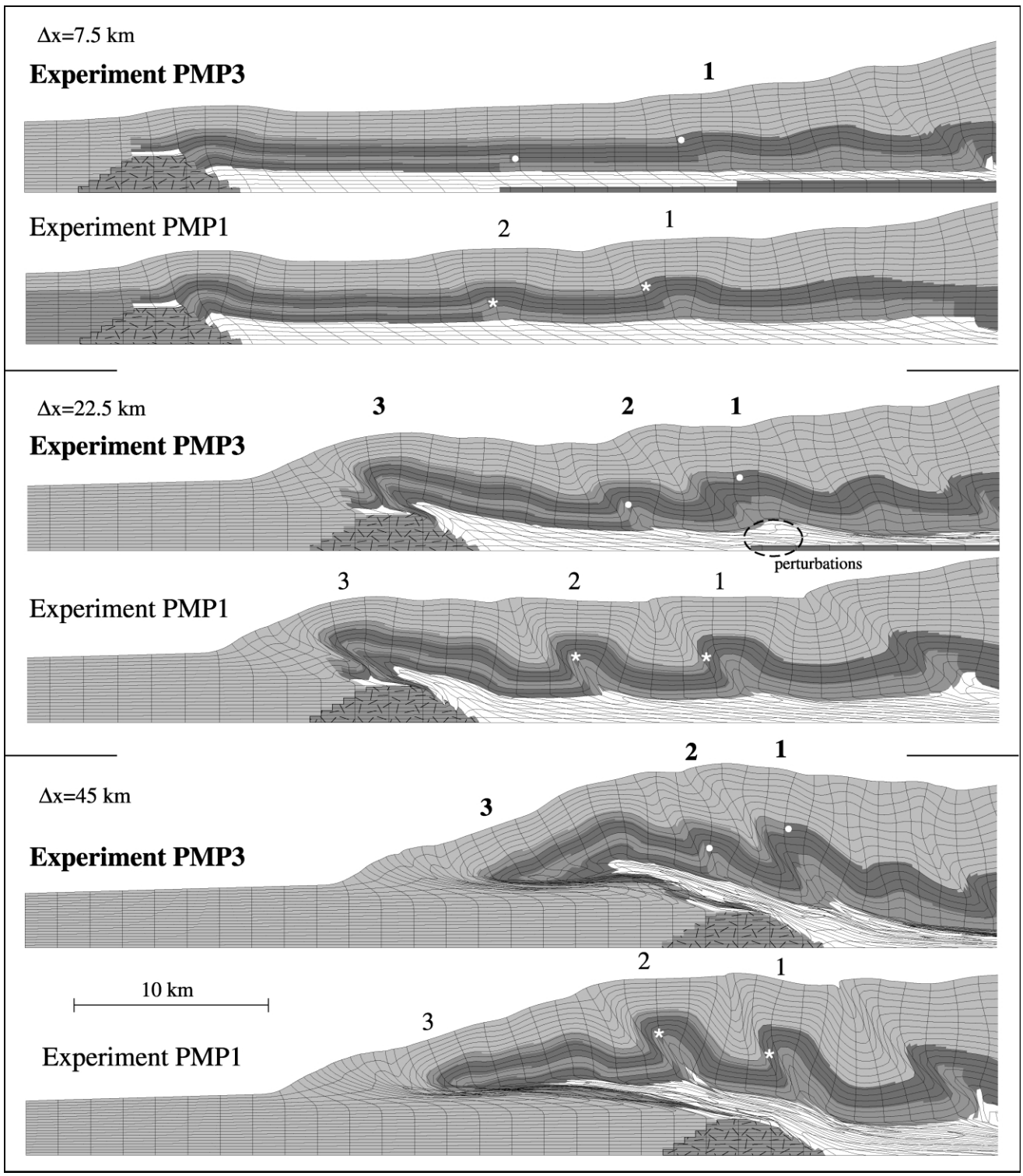

Fig. 11. Sections of experiment PMP3 and PMP1 at different stages of convergence. Areas shown vary from: 28–73 km (7.5 km of convergence), to 18–61 km (22.5 km of convergence), to 1–46 km (45 km of convergence). 1, 2, 3: numbers of folds initiated from hinterland to the foreland. White dot: positions of layer irregularities in experiment PMP3, white asterisk: positions of layer irregularities in experiment PMP1.

of competent model carbonates inclined towards the foreland, which leads to a gradual decrease in the thickness of the weak linear viscous layer in the direction of the hinterland (Fig. 12). After 7.5 km of convergence, the experiment shows a similar pattern of initial anticlines as experiment PMP3, which may be explained by the same average thicknesses of weak detachment material. As deformation continues (22.5 and 45 km of convergence), shear strain is localized in the forelimbs of folds. The concentration of shearing in the forelimb of folds **1** and **2** is even more intense than in experiment PMP1 and it

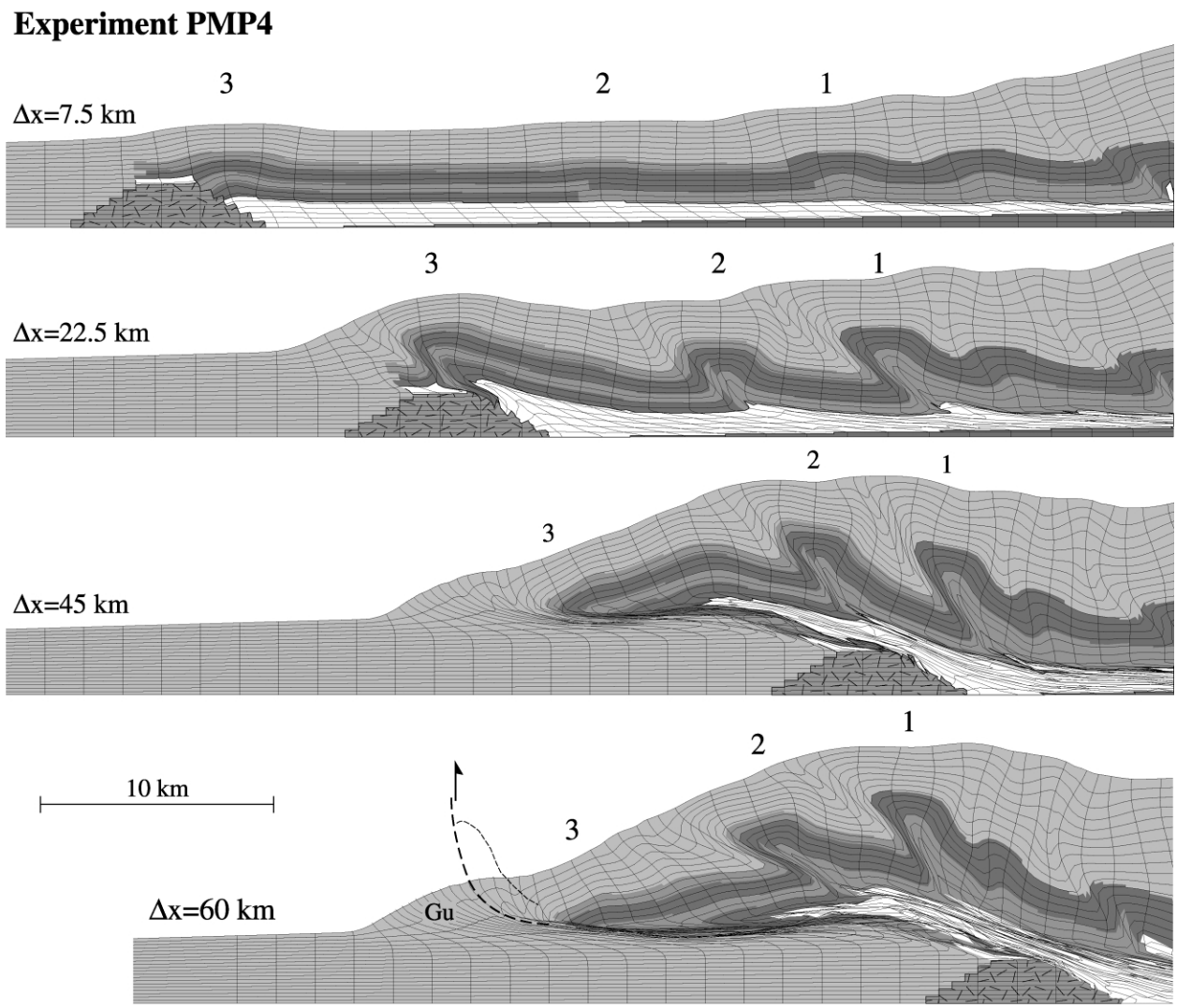

Fig. 12. Sections of experiment PMP4 at different stages of convergence. Areas shown extend from: 28–73 km (7.5 km of convergence), to 18–61 km (22.5 km of convergence), to 1–46 km (45 km of convergence), to 0–40 km (60 km of convergence). 1, 2, 3: numbers of folds initiated from hinterland to the foreland. Gu: Gurnigel nappe. Dashed lines: interpreted traces of Klippen nappe basal thrust and frontal fold after thrusting over the Gurnigel nappe.

occurs at the discontinuities. The reduced thickness of the weak detachment material beneath these folds causes a higher amount of foreland vergent thrusting, as observed in the simple generic models presented in Wissing et al. (2002). The smooth basement ramp does not generate stress concentrations. Thus the wavelength pattern is not disturbed. The initial anticlines become amplified, and the discontinuities at the model paleofaults are used to localize shear strain.

The pattern of folds and related thrusts of models PMP3 and PMP4 are similar to the ones observed in the Médianes Plastiques. We thus conclude that the decreasing thickness of the weak detachment horizon in the Klippen nappe paleobasin from foreland to hinterland may be a realistic assumption. Additionally, the gradual, linear decrease in sediment thickness below the weak detachment horizon used for model PMP4 produces structures that resemble the natural analogue closely.

In all experiments, the rigid horst (MMM basement high) at the far end of the multilayered sequence has an important influence on the evolution of nappe deformation owing to the lateral limits of the weak detachment horizon. It forms a backstop for the forward propagation of deformation and leads to thrusting of the fold train on top of the sediments on the far side of the basement high. Furthermore, the basement high is responsible for tectonic thinning of detachment material and the original cover of the high during the transport of the model cover nappe across it, which results in a larger localization of deformation in thrust faults and the formation of a mélange zone at the base of the model nappe.

After 60 km of displacement in the model of experiment PMP4 (Fig. 12, bottom) the following first order characteristics are shared with the Médianes Plastiques: (a) folds **1** and **2** show thrust faults in their forelimbs at positions of former paleofaults, as is the case for sectors B and C of the Klippen nappe (Fig. 3); (b) folds **1** and **3**, apart from the sheared forelimbs, are simple structures and flanked by

deep, also simply structured synclines on the external side; and (c) fold **3** develops a mélange zone at the thrust contact to the underlying units.

Fold **3** of experiment PMP4 is recumbent, whereas the frontal fold of the Klippen nappe has a vertical backlimb and has overthrust the Gurnigel nappe. As mentioned earlier, the Gurnigel nappe forms the most external part of the Nappe Supérieure, which was overridden by the structurally lower Klippen nappe in the latest phase of its emplacement. If, in experiment PMP4, we envisage a 'break-through' of the basal thrust below fold **3** (as indicated by the dashed curve and the arrow in Fig. 12), the frontal part of the model Klippen nappe would end up overthrusting the frontal part of the model Nappe Supérieure. Owing to model resolution, experiments are not able to include such complex out-of-sequence thrusting. It is, however, easy to imagine that heterogeneities within the model Nappe Supérieure could cause a 'break-through' and associated out-of-sequence thrusting. Such a heterogeneity could be envisaged by the thick turbidite sequence of the Gurnigel nappe, which contrasts with the mélange of the more internal parts of the Nappe Supérieure.

4. Summary and conclusions

In this study we compare data from field observations with results from numerical forward modelling designed to gain insight into the dynamics of large scale deformation and emplacement of cover nappes. Individual model experiments have multilayered characteristics resembling those obtained from a reconstruction of the Klippen nappe paleobasin. However, the results can also be interpreted with respect to the general behaviour of cover nappes with complex inherited basin geometries. We summarize the primary conclusions drawn from this work as follows:

1. Discontinuous detachment horizons can control positions of thrust ramps, which trigger the stacking of imbricates in cover nappes. In the case of the Klippen nappe, thin middle Triassic evaporites, disrupted by Jurassic normal faults below the thick massive carbonate sequences of the Préalpes Médianes Rigides may have led to the decoupling and stacking of one large and one or two smaller imbricates in the study area.
2. Lateral layer heterogeneities resulting from paleofaults are preferred positions for the initiation of folds and control the wavelength pattern of a fold train. In the study area, thrust faults are in fact located at abrupt lateral thickness and facies changes within the multilayered carbonate sequences.
3. Steps in the competent rocks underlying the detachment horizon cause stress perturbations and experiments suggest that these affect the distinct wavelength pattern produced by the initiation of anticlines at layer irregularities. The perturbations are even able to suppress the localization of folds related to paleofaults (conclusion 2). In the Klippen nappe, we observe that folds are in fact associated with paleofaults and we may thus conclude that there is smooth carbonate surface at the base of the detachment horizon, which does not include significant basement steps. Consequently, we suggest that in the Préalpes Médianes Plastiques smaller-scale paleofaults did not root into the Triassic carbonate layers below, but flattened within the weak evaporite horizon. A similar pattern of extensional faults is reported from the Atlantic passive margin off Morocco, where the Cretaceous clastic and carbonate sequences are cut by listric normal faults levelling off in the lower Cretaceous clastics (Heymann, 1989).
4. The Môle–Moléson–Mythen (MMM) basement high at the foreland end of the Klippen nappe paleobasin, at which the mechanically weak layer terminates, provided a resistance to push from behind and facilitated the thrusting of the Klippen nappe on top of the neighbouring realm (Niesen nappe). In the experiments it also leads to the formation of a recumbent fold and a tectonic thinning of the cover of the 'basement' high and adjacent areas. Ultimately, a mélange zone develops at the base of the model Klippen nappe. This behaviour resembles the observation of small fragments, which occur along the basal thrust of the Klippen nappe and other Alpine-type cover nappes (see e.g. Wissing and Pfiffner, 2002). The fault-related folds in the Médianes Plastiques may partly be a result of the tectonically thinned detachment layer after transport of the fold train across a rigid high at the external basin front.

Acknowledgements

This project was funded by the Swiss National Science Foundation (grant no. 20-55411.98). We thank C. Beaumont and the Geodynamics Group of the Dalhousie University for permission to use their finite element code and S. Ellis for stimulating discussions and useful suggestions that improved the manuscript.

References

Argand, E., 1911. Les nappes de recouvrement des Alpes Pennines et leurs prolongement structuraux. Matériaux Carte géologique Suisse (n.s.) 31.

Baud, A., Septfontaine, M., 1980. Présentation d'un profil palinspastique de la nappe des Préalpes Médianes en Suisse occidentale. Eclogae Geologicae Helveticae 73 (2), 651–660.

Beaumont, C., Kamp, P.J.J., Hamilton, J., Fullsack, P., 1996. The continental collision zone, South Island, New Zealand: comparison of geodynamic models and observations. Journal of Geophysical Research 101, 3333–3359.

Bill, M., Bussy, F., Cosca, M., Masson, H., Hunziker, J.C., 1997. High precision U-Pb and $^{40}Ar/^{39}Ar$ dating of an Alpine ophiolite (Gets nappe, French Alps). Eclogae Geologicae Helveticae 90 (1), 43–54.

Boller, K., 1963. Stratigraphische und Mikropaläontologische

Untersuchungen im Neocom der Klippendecke. Eclogae Geologicae Helvetiae 56, 15–102.

Butler, R.W.H., 1989. The influence of pre-existing basin structure on thrust system evolution in the Western Alps. In: Cooper, M.A., Williams, G.D. (Eds.), Inversion Tectonics. Geological Society of London Special Publication 44, pp. 105–122.

Caron, C., 1972. La Nappe Supérieure des Préalpes: subdivisions et principaux caractères du sommet de l'édifice préalpin. Eclogae Geologicae Helvetiae 65/1, 57–73.

Caron, C., Homewood, P., Morel, R., Stuijvenberg, J., 1980. Témoins de la nappe du Gurnigel sur les Préalps. Médianes: une confirmation de son origine ultrabriançonnaise. Bulletin de la Société Fribourgeoise des Sciences Naturelles 69, 64–79.

Chester, J.S., Logan, J.M., Spang, J.H., 1991. Influence of layering and boundary conditions on fault-bend and fault-propagation folding. Geological Society of America Bulletin 103, 1059–1072.

Currie, J.B., Patnode, H.W., Trump, R.P., 1962. Development of folds in sedimentary strata. Geological Society of America Bulletin 73, 655–674.

Dall'Agnolo, S., 1997. Die Kreide und das Tertiär der Brekziendecke in den Französischen und Schweizer Voralpen: Stratigraphie, Sedimentologie und Geodynamik. Ph.D. thesis, University of Fribourg (Switzerland).

Davis, D.M., Engelder, T.E., 1985. The role of salt in fold-and-thrust belts. Tectonophysics 119, 67–88.

Epard, J.-L., Escher, A., 1996. Transition from basement to cover: a geometric model. Journal of Structural Geology 18, 533–548.

Escher, A., 1988. Structure de la nappe du Grand Saint-Bernard entre le val de Bagnes et les Mischabel. Geologische Berichte 7, Landeshydrologie und -geologie, Bern.

Escher, A., Masson, H., Steck, A., 1993. Nappe geometry in the Western Alps. Journal of Structural Geology 15, 501–509.

Fermor, P.R., Moffat, I.W., 1992. Tectonics and structure of the Western Canada foreland basin. In: Macqueen, R.W., Leckie, D.A. (Eds.), Foreland Basins and Fold Belts. AAPG Memoir 55, pp. 81–105.

Fischer, M.P., Woodward, N.B., 1992. The geometric evolution of foreland thrust systems. In: McClay, K.R., (Ed.), Thrust Tectonics, Chapman & Hall, pp. 181–189.

Fullsack, P., 1995. An arbitrary Lagrangian–Eulerian formulation for creeping flows and its application in tectonic models. Geophysical Journal International 120, 1–23.

Handin, J., 1969. On the Coulomb–Mohr failure criterion. Journal of Geophysical Research 74, 5343–5348.

Heymann, M.A.W., 1989. Tectonic and depositional history of the Moroccan continental margin. In: Tankard, A.J., Balkwill, H.R. (Eds.), Extensional Tectonics and Stratigraphy of the North Atlantic Margins. AAPG Memoir 46, pp. 323–340.

Jaboyedoff, M., Thélin, P., 1996. New data on low-grade metamorphism in the Briançonnais domain of the Prealps, Western Switzerland. European Journal of Mineralogy 8, 577–592.

Jamison, W.R., 1987. Geometric analysis of fold development in overthrust terranes. Journal of Structural Geology 9, 207–219.

Johnson, A.M., 1980. Folding and faulting of strain-hardening sedimentary rocks. Tectonophysics 62, 251–278.

Lemoine, M., Bas, T., Arnaud-Vanneau, A., Arnaud, H., Dumont, T., Gidon, M., Bourbon, M., de Graciansky, P.-C., Rudkiewicz, J.-L., Megard-Galli, J., Tricarl, P., 1986. The continental margin of the Mesozoic Tethys in the Western Alps. Marine and Petroleum Geology 3, 179–199.

Lugeon, M., Gagnebin, E., 1941. Observations et vues nouvelles sur la géologie des Préalpes romandes. Bulletin des Laboratoires de Géologie, Minéralogie, Géophysique et du Musée Géologique de l'Université de Lausanne 72, 1–90.

Marthaler, M., 1998. Le Cervin est-il africain? Histoire géologique de la formation des Alpes. Paysages Découverts 3, Université de Lausanne.

Masson, H., 1976. Un siècle de géologie des Préalpes: de la découverte des nappes à la recherche de leur dynamique. Eclogae Geologicae Helvetiae 69/2, 527–575.

Mosar, J., 1988. Métamorphisme transporté dans les Préalpes. Schweizer Mineralogische und Petrographische Mitteilungen 68, 77–94.

Mosar, J., 1989. Déformation interne dans les Préalpes médianes (Suisse). Eclogae Geologicae Helvetiae 82/3, 765–793.

Mosar, J., 1991. Géologie structurale dans les Préalpes médianes (Suisse). Eclogae Geologicae Helvetiae 84/3, 689–725.

Mosar, J., 1997. Folds and thrusts in the Préalps Médianes Plastiques Romandes. Bulletin de Société vaudoise des Sciences naturelles 84/4, 347–384.

Mosar, J., Borel, G., 1992. Paleostress from the Préalpes Médianes (Switzerland). Annales Tectonicae VI, 115–133.

Mosar, J., Stampfli, G.M., Girod, F., 1996. Western Préalpes Médianes Romandes: timing and structure. A review. Eclogae Geologicae Helvetiae 89/1, 389–425.

Pfiffner, O.A., 1993. The structure of the Helvetic Nappes and its relation to the mechanical stratigraphy. Journal of Structural Geology 15, 511–521.

Pfiffner, O.A., Lehner, P., Heitzmann, P.Z., Mueller, S., Steck, A. (Eds.), 1997. Deep Structure of the Swiss Alps—Results from NRP 20. Birkhäuser Verlag AG, Basel.

Plancherel, R., 1979. Aspects de la déformation en grand dans les Préalpes médianes plastiques entre Rhône et Aar. Implications cinématiques et dynamiques. Eclogae Geologicae Helvetiae 72/1, 145–214.

Rodgers, J., 1950. Mechanics of Appalachian folding as illustrated by Sequatchie Anticline, Tennessee and Alabama. Bulletin of the American Association of Petroleum Geologists 34, 672–681.

Sartori, M., 1987. Structure de la Zone du Combin entre les Diablons et Zermatt (Valais). Eclogae Geologicae Helvetiae 80, 789–814.

Sartori, M., 1990. L'unité du Barrhorn (Zone pennique, Valais, Suisse). Mémoires de Géologie (Lausanne) 6, 1–156.

Sassi, W., Colletta, B., Balé, P., Paquereau, T., 1993. Modelling of structural complexity in sedimentary basins: the role of pre-existing faults in thrust tectonics. Tectonophysics 226, 97–112.

Schedl, A., Wiltschko, D.V., 1987. Possible effects of pre-existing basement topography on thrust fault ramping. Journal of Structural Geology 9, 1029–1037.

Shreve, R.L., Cloos, M., 1986. Dynamics of sediment subduction, melange formation and prism accretion. Journal of Geophysical Research 91, 10229–10245.

Stampfli, G.M., 1993. Le Briançonnais, terrain exotique dans les Alpes. Eclogae Geologicae Helvetiae 86, 1–45.

Stampfli, M., Marthaler, M., 1990. Divergent and convergent margins in the North-Western alps confrontation to actualistic models. Geodinamica Acta 4, 159–184.

Trümpy, R., 1960. Paleotectonic evolution of the Central and Western Alps. Geological Society of America Bulletin 71, 843–908.

von der Weid, J., 1961. Géologie des Préalpes médianes au SW du Moléson. Ph:D. thesis, University of Fribourg (Switzerland).

Willis, B., 1893. The mechanics of Appalachian structure. United States Geological Survey Annual Report 13/2, 211–281.

Wiltschko, D.V., 1981. Thrust sheet deformation at a ramp: summary and extension of an earlier model. In: McClay, K.R., Price, N.J. (Eds.), Thrust and Nappe Tectonics. Geological Society of London Special Publication 9, pp. 55–63.

Wiltschko, D.V., Eastman, D., 1983. Role of basement warps and faults localizing thrust fault ramps. Geological Society of America Memoir 158, 177–190.

Wiltschko, D.V., Eastman, D.B., 1988. A photoelastic study of the effects of preexisting reverse faults in basement on the subsequent deformation of the cover. Geological Society of America Memoir 171, 111–118.

Wissing, S.B., Pfiffner, O.A., 2002. The Klippen Nappe between Gantrisch, Schwarzsee and Spillgerte: implications for its Alpine tectonic evolution. Eclogae Geologicae Helvetiae 95 (3), 381–399.

Wissing, S.B., Ellis, S., Pfiffner, O.A., 2002. Numerical models of Alpine-type cover nappes. Tectonophysics in press.

Woodward, N.B., 1988. Primary and secondary basement controls on thrust sheet geometries. Geological Society of America Memoir 171, 353–366.

Woodward, N.B., Rutherford, E. Jr, 1989. Structural lithic units in external orogenic zones. Tectonophysics 158, 247–267.